

## ENERGY ABSORPTION ABILITIES OF EPOXIDE COMPOSITES STRENGTHEN BY GLASS AND CARBON FIBRES

Stanisław Ochelski, Paweł Gotowicki, and Andrzej Kiczko

Military University of Technology  
2 Kaliski Str, 00-908 Warszawa, Poland  
tel.: +48 22 683 85 48, +48 22 683 72 21, tel./fax: +48 22 683 94 61  
e-mail: p.gotowicki@wme.wat.edu.pl, andrzej.kiczko@wat.edu.pl

### Abstract

The paper presents an experimental work pertaining to the energy absorption capability of FRP specimens. The tests were performed on the INSTRON 8802 universal testing machine and the energy absorbed by the structure was calculated from the load-shortening diagram. A series of experiments were performed for composite thin walled tubes and cones with different semi-vertex angles ranging from 5° to 20°. The specimens were made of epoxy (E-53) and vinylester (VE-2MM) composites with glass, carbon and aramid fibers in three forms: filament yarn, fabric and mat. The influence of specimen geometry, fiber orientation and composite structure on the energy absorbing capability was studied.

In particular relative energy of absorption (WEA) in dependence on materials, typical dependence of a crushing force on displacements (shortenings), comparison of mechanical properties of epoxide, monotropic composites strengthen with glass and carbon fibres, comparison of mechanical properties of epoxide, orthotropic composites strengthen with glass and carbon materials, dependence of the destructive strength on displacement of carbon/epoxide composite, progressive destruction of a specimen made of carbon/epoxide composite, mechanism of destruction by layer bending, influence of the thickness of the cone wall on the ability of absorbing energy by the epoxide composite, dependence of WEA on the angle  $\alpha$  for the chosen structures of composites are presented in the paper.

**Keywords:** energy absorption, FRP, experimental investigation

### 1. Introduction

Energy absorbing constructions are able to seize kinetic energy during an impact, which negative increment is equivalent to a destruction work (crushing, breaking) of the construction.

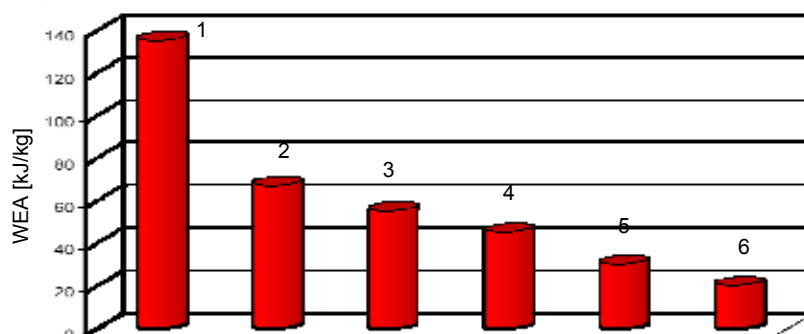


Fig. 1. Relative energy of absorption (WEA) in dependence on materials: 1 - carbon/PEEK, 2 - carbon/epoxide, 3 - glass/epoxide, 4 - short glass fibres/epoxide, 5 - steel, 6 - aluminium, after Ref. 7

Nowadays, energy absorbing constructions are widely used, among others, in aeronautical industry (they minimize effects of crash landings), in constructions of containers destined to airdrops from planes, in protective systems against effects of explosions of blowing charges, in

automotive industry (especially in race cars), in railways they are used, among others, for containers carrying fuels or caustics. In aeronautics, for energy absorbing constructions, taking into account the demanded lightness of constructions, polymer composites of various kinds, shapes and forms of strengthening are used. Polymer composites have not only the highest relation of strength and stiffness to density ( $R/\rho$ ,  $E/\rho$ ) but also the highest relative energy of absorption (energy of absorption related to mass), in comparison with metals and their alloys (Fig. 1).

The destruction of energy absorbing constructions cannot be done rapidly, as it takes place in the beam destruction at global buckling, for sake of enabling energy absorbing constructions to absorb an impact energy efficiently, the process of destruction should take place progressively so as to crush (destruct) each volume of a specimen into smallest particules. The typical diagram of a such dependence is presented in Fig. 2.

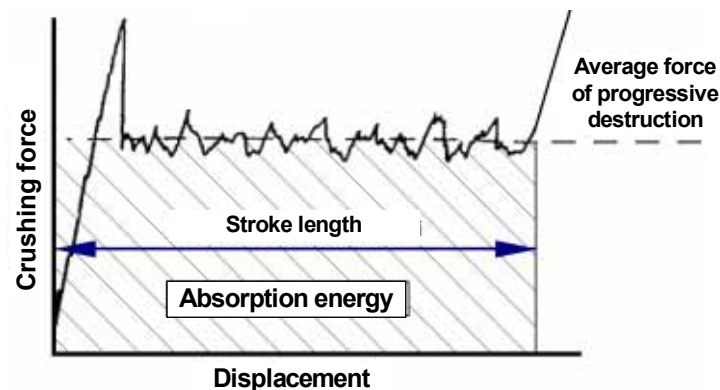


Fig. 2. Typical dependence of a crushing force on displacements (shortenings)

The process of progressive destruction mainly depends on mechanical properties of fibres, kinds of strengthening structures, fibre orientation in a layer, a sequence of layer arrangement, the fibre content in a composite and on a shape and geometry of specimens.

## 2. Subject and Method of Investigations

The subject of investigations were specimens made from epoxide composites (E-53), strengthen by glass fibres in shapes of: STR-012-350-110 rowing fabric of  $350 \text{ g/m}^2$ , ES-10-400-0-60 rowing strips, and a glass mat of  $316 \text{ g/m}^2$ . Epoxide composites strengthen by carbon fibres in shape of TENAX HTA 5131 rowing fabric and a monotropic composite strengthen by stripes of TENAX HTS 5631 carbon rowing.

Mechanical properties of composites were described in experimental investigations which were carried out according to standards: PN-EN ISO 527-1:1998, PN-EN ISO 527-2:1998, ASTM-3039-76, ISO 8515:91, ISO 3597-3:93, ASTM D 3410-75, ISO 14129:1997 and guidelines from [2]. The results are presented in Tab. 1.

The specimens in the shape of pipes of internal diameter  $D_i = 49.3 \text{ mm}$  and the height  $h = 100 \text{ mm}$  and in shapes of truncated cones with a semi vertical angle  $\alpha = 5, 10, 15$  and  $20^\circ$  and a height  $h = 90 \text{ mm}$  and the thickness of the wall  $t = 2, 3, 4, 5, 6$  and  $7 \text{ mm}$  (Fig. 3), were taken to the investigations to test their absorbing abilities. Specimens in the shape of pipes, on one of the edges, have bevels under the angle of  $60^\circ$ , fulfilling the function of an initiator of destruction, which cause significant reduction of  $P_{\max}$ . Specimens in shapes of truncated cones do not need the initiator because the beginning of destruction starts with smaller diameter of a cone where the highest stresses occur.

On the principle of data from literature and results of our investigations the following structures of specimens were taken into testing:  $[0_n]$ ;  $[90_n]$ ;  $[(0/90)_T]_n$ ;  $[90/0_n/90]$ ;  $[\pm 15/0_n/\pm 15]$ ;

$[\pm 30/0_n/\pm 30]$ ;  $[(\pm 45)_T/0_n/(\pm 45)_T]$ ;  $[(0/90)_T/0_n/(0/90)_T]$ ;  $[(\pm 45)_T/(0/90)_T/(\pm 45)_T]$ ; where the layer  $[0^\circ]$  stands for a composite with continuous fibres arranged parallel to the axis of a specimen;  $[90^\circ]$  – fibres are arranged orthogonal to the axis of a specimen;  $[(0/90)_T]$  – the layer strengthened by the material. Middle layers of specimen walls, have usually fibres arranged parallel to the axis of a specimen. The specimens from composites strengthened with a glass mat were also tested. Testing were carried out on a standard machine ISTRON 8802 at temperature of  $20^\circ\text{C}$  and humidity of 55%. The speed of loading (the speed of machine’s traverse) during tests equalled to 0.66 mm/s. Dependence of the destruction force on strain (a specimen’s contraction) and other measured values, received during testing, were automatically registered. Moreover, in Tables 2 and 3 characteristic specimen dimensions, presented in Fig. 4, are given.

### 3. Results of Experiments

Results of experiments on mechanical properties of epoxide composites strengthened by carbon and glass fibres are presented in Tables 1a and 1b and the denotation of established directions of monotropic and orthotropic composite are shown in Fig. 3. Specific mechanical properties are necessary to the numerical simulation of progressive destruction of a composite.

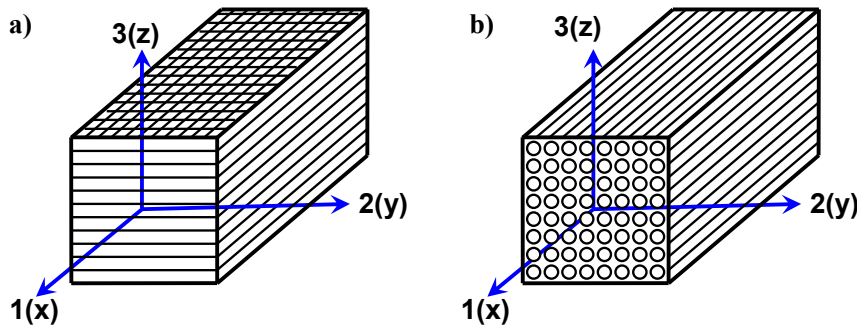


Fig. 3 Directions of composite strengthening a) orthotropic composite, b) monotropic

Tab. 1a. Comparison of mechanical properties of epoxide, monotropic composites strengthened with glass and carbon fibres

L.p		Values described in tests	Composite carbon/epoxide	Composite glass/epoxide	Unit
1	$E_1^+$	Young modulus, tension in the direction 1	91.04	35.21	[GPa]
2	$E_1^-$	Young modulus, compression in the direction 1	88.9	41.1	[GPa]
3	$\nu_{12}$	Poisson’s ratio in the plane 1-2	0.27	0.311	[-]
4	$G_{12}$	Modulus of volume elasticity in the plane 1-2	3.6	2.27	[GPa]
5	$R_1^+$	Tensile strength in the direction 1	1004.9	665.1	[MPa]
6	$R_1^-$	Compression strength in the direction 1	578.7	412	[MPa]
7	$T_{12}$	Shear strength in the plane 1-2	39.1	61.1	[MPa]
8	$\epsilon_1^+$	Destructive strains, tension in the direction 1	0.011	0.02	[-]
9	$\epsilon_1^-$	Destructive strains, compression in the direction 1	0.0065	0.011	[-]
10	$\gamma_{12}$	Destructive strains, shearing in the plane 1-2	0.027	0.035	[-]

Tab. 1b. Comparison of mechanical properties of epoxide, orthotropic composites strengthen with glass and carbon materials

L.p	Values described in tests		Composite carbon/epoxide	Composite glass/epoxide	Unit
1	$E_1^+$	Young modulus, tension in the direction 1	46.4	19.54	[GPa]
2	$E_1^-$	Young modulus, compression in the direction 1	50.6	19.33	[GPa]
3	$\nu_{12}$	Poisson's ratio in the plane 1-2	0.14	0.143	[-]
4	$G_{12}$	Modulus of volume elasticity in the plane 1-2	2.91	2.92	[GPa]
5	$R_1^+$	Tensile strength in the direction 1	468.6	311.7	[MPa]
6	$R_1^-$	Compression strength in the direction 1	375.2	306	[MPa]
7	$T_{12}$	Shear strength in the plane 1-2	57.03	38.4	[MPa]
8	$\epsilon_1^+$	Destructive strains, tension in the direction 1	0.0101	0.018	[-]
9	$\epsilon_1^-$	Destructive strains, compression in the direction 1	0.0074	0.016	[-]
10	$\gamma_{12}$	Destructive strains, shearing in the plane 1-2	2.17	3.22	[-]

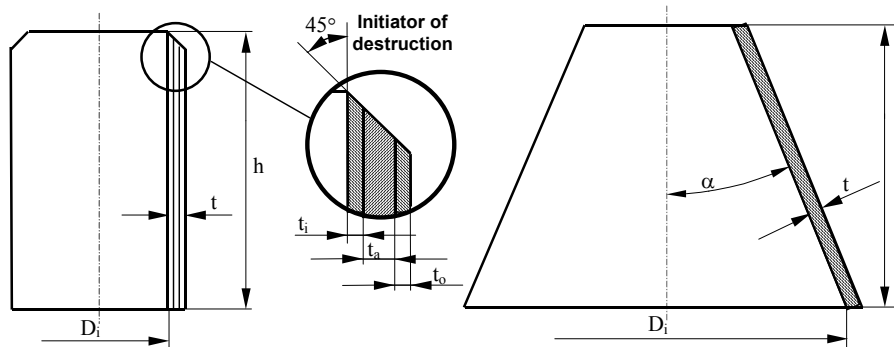


Fig. 4. Shapes of specimens used in tests

Results of tests as an average from few tests, specified in Tables 2 i 3, they mark characteristic values which stand for:

$P_{max}$  -maximal crushing strength, it is the first peak on the curve  $P - \Delta l$ , which shows the beginning of the destruction;

EA -absorbed energy of impact, equals to the surface (field) under the curve  $P - \Delta l$ ;

$P_a$  -average force, which is equal to ( $P_a = EA/\Delta l_{max}$ );

WEA -Relative absorbed energy  $WEA = EA/m_p$  – where  $m_p$  is the mass of a part of the destructed specimen;

$\alpha$  -half cone angle;

t -thickness of the wall;

$D_i$  -internal diameter (for a cone, the diameter of a greater base);

$t_i$  -thickness of internal layer;

$t_a$  -thickness of the middle layer;

$t_o$  -thickness of external layer;

h -the height of a specimen;

z -weight-content of fibres in a composite;

m -specimen mass;

g -index of unity of strength ( $P_{max}/P_{min}$ ).

Dependence of the destructive strength on displacement for specimens made of composites strengthened with carbon and glass fibres, specified in tests, is presented, as an example, in Figs. 5 and 9. Whereas, the complete results of tests, presented in Tabs. 2 and 3 are grouped depending on the thickness of a wall and the shape of a specimen and the composite structure.

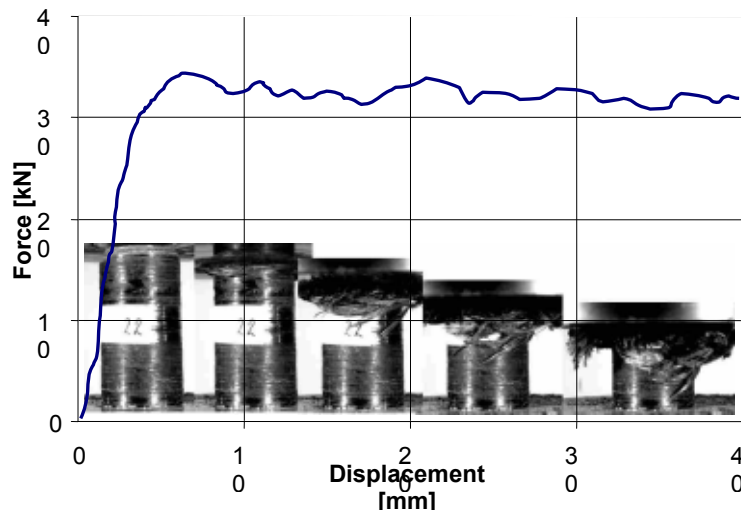


Fig. 5 Dependence of the destructive strength on displacement of carbon/epoxide composite

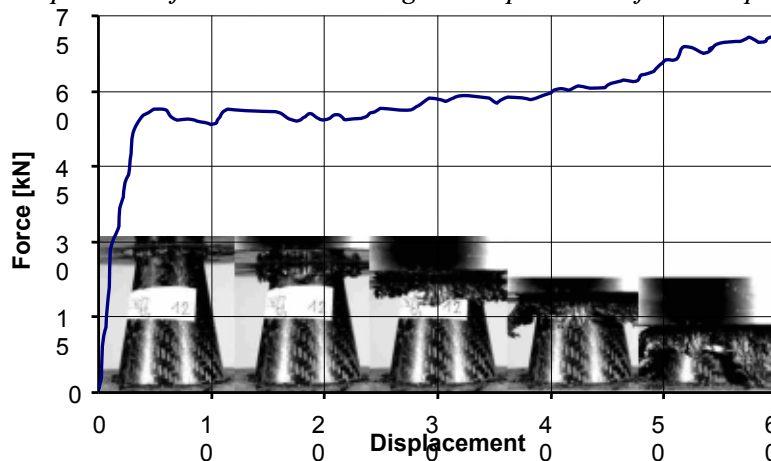


Fig. 6. Progressive destruction of a specimen made of carbon/epoxide composite

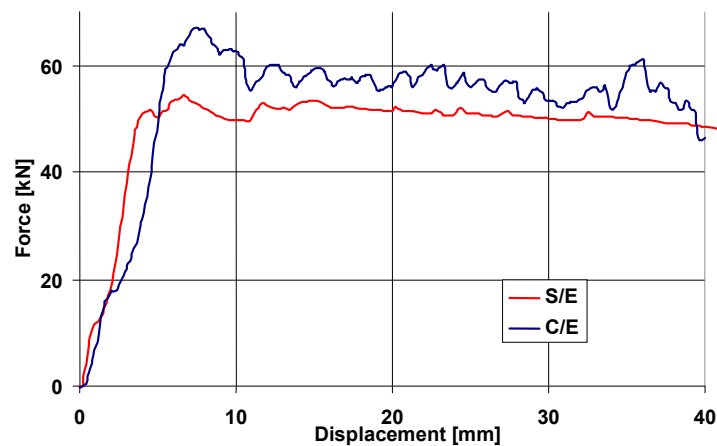


Fig. 7. P-Δ dependence for pipes with 90<sub>2</sub>/0<sub>2</sub>/90<sub>2</sub> structure made of glass/epoxide and carbon/epoxide composite



Tab. 2. Properties of specimens made of a composite carbon/epoxide

No of specimen	Structure	$\alpha$ [°]	t [mm]	$D_i$ [mm]	$t_i$ [mm]	$t_a$ [mm]	$t_o$ [mm]	h [mm]	z [%]	m [g]	$P_{max}$ [kN]	$P_a$ [kN]	$\frac{P_{max}}{P_{sr}}$	EA [J]	WEA [kJ/kg]
1	(0/90) <sub>T</sub> /0/(0/90) <sub>T</sub>	5	1.2	59.5	0.4	0.4	0.4	75.0	42	22.8	24.4	21.4	0.877	1602	70.3
2	(0/90) <sub>T</sub> /0 <sub>2</sub> /(0/90) <sub>T</sub>	5	2.0	59.4	0.5	1.0	0.5	85.6	42	39.5	39.5	32.3	0.818	2761	69.9
3	(0/90) <sub>T</sub> /0 <sub>3</sub> /(0/90) <sub>T</sub>	5	2.2	59.5	0.4	1.4	0.4	83.4	42	42.2	46.2	34.7	0.751	2896	68.6
4	(0/90) <sub>T</sub> /0/(0/90) <sub>T</sub>	10	1.2	59.4	0.4	0.4	0.4	78.8	42	21.5	21.5	17	0.791	1336	62.2
5	(0/90) <sub>T</sub> /0 <sub>2</sub> /(0/90) <sub>T</sub>	10	2.4	59.7	0.6	1.2	0.6	83.6	42	41.3	44.8	35.1	0.783	2924	70.8
6	(0/90) <sub>T</sub> /0 <sub>3</sub> /(0/90) <sub>T</sub>	10	3.2	59.8	0.6	2.0	0.6	84.9	42	71.0	72.8	58.4	0.802	4924	69.4
7	(0/90) <sub>T</sub> /0/(0/90) <sub>T</sub>	15	1.2	58.8	0.4	0.4	0.4	54.1	42	17.4	18.1	16.5	0.912	892	51.3
8	(0/90) <sub>T</sub> /0 <sub>2</sub> /(0/90) <sub>T</sub>	15	2.0	59.2	0.5	1.0	0.5	58.0	42	23.7	27.3	22.8	0.835	1322	55.8
9	(0/90) <sub>T</sub> /0 <sub>3</sub> /(0/90) <sub>T</sub>	15	3.2	58.9	0.6	2.0	0.6	62.4	42	42.0	52.5	38.9	0.741	2426	57.8
10	(0/90) <sub>T</sub> /0/(0/90) <sub>T</sub>	20	1.2	79.5	0.4	0.4	0.4	67.0	42	25.2	14.7	13.6	0.925	911	36.4
11	(0/90) <sub>T</sub> /0 <sub>2</sub> /(0/90) <sub>T</sub>	20	2.0	78.8	0.5	1.0	0.5	68.9	42	36.0	27.9	22.5	0.806	1552	43.1
12	(0/90) <sub>T</sub> /0 <sub>3</sub> /(0/90) <sub>T</sub>	20	2.5	79.5	0.5	1.5	0.5	68.4	42	49.9	40	34.7	0.868	2373	47.6
13	(0/90) <sub>T</sub> /0/(0/90) <sub>T</sub>	0	1.7	39.3	0.6	0.5	0.6	98.2	42	28.5	27.7	21.1	0.762	2075	70.9
14	(0/90) <sub>T</sub> /0 <sub>2</sub> /(0/90) <sub>T</sub>	0	2.3	39.3	0.6	1.1	0.6	98.0	42	35.6	32.2	25.4	0.789	2489	71.0
15	(0/90) <sub>T</sub> /0 <sub>3</sub> /(0/90) <sub>T</sub>	0	3.0	39.3	0.6	1.8	0.6	102.2	42	54.6	54.5	39.4	0.723	4027	71.6
16	[(0/90) <sub>T</sub> ] <sub>2</sub> /0 <sub>2</sub> /[(0/90) <sub>T</sub> ] <sub>2</sub>	0	3.0	39.3	1.0	1.0	1.0	80.2	41	41.6	65.1	49	0.753	2586	87.4
17	[(0/90) <sub>T</sub> ] <sub>2</sub> /0 <sub>2</sub> /[(0/90) <sub>T</sub> ] <sub>2</sub>	5	2.1	59.5	0.7	0.7	0.7	76.3	41	35.7	43.9	35.67	0.813	2722	76.2
18	[(0/90) <sub>T</sub> ] <sub>2</sub> /0 <sub>2</sub> /[(0/90) <sub>T</sub> ] <sub>2</sub>	10	2.1	59.8	0.7	0.7	0.7	77.3	41	36.4	45.8	37.25	0.813	2879	79.1
19	[(0/90) <sub>T</sub> ] <sub>2</sub> /0 <sub>2</sub> /[(0/90) <sub>T</sub> ] <sub>2</sub>	15	2.1	59.3	0.7	0.7	0.7	50.6	41	24	64.2	36.16	0.563	1830	76.2
20	[(0/90) <sub>T</sub> ] <sub>2</sub> /0 <sub>2</sub> /[(0/90) <sub>T</sub> ] <sub>2</sub>	20	2.4	79.4	0.8	0.8	0.8	66.1	41	50.4	68.3	48.58	0.711	3211	63.7
21	[(0/90) <sub>T</sub> ] <sub>3</sub> /0 <sub>2</sub> /[(0/90) <sub>T</sub> ] <sub>3</sub>	0	3.6	39.3	1.4	0.8	1.4	81.2	42	50.1	67.5	52.34	0.775	4250	84.5
22	[(0/90) <sub>T</sub> ] <sub>3</sub> /0 <sub>2</sub> /[(0/90) <sub>T</sub> ] <sub>3</sub>	5	2.9	59.2	1.1	0.7	1.1	83.5	42	49.4	57.8	45.92	0.794	3834	77.6
23	[(0/90) <sub>T</sub> ] <sub>3</sub> /0 <sub>2</sub> /[(0/90) <sub>T</sub> ] <sub>3</sub>	10	2.9	60.1	1.1	0.7	1.1	82.8	42	53.5	57.7	49.43	0.857	4093	76.5
24	[(0/90) <sub>T</sub> ] <sub>3</sub> /0 <sub>2</sub> /[(0/90) <sub>T</sub> ] <sub>3</sub>	15	3.2	59.3	1.2	0.8	1.2	58.7	42	44.5	72.1	56.41	0.782	3311	74.4
25	[(0/90) <sub>T</sub> ] <sub>3</sub> /0 <sub>2</sub> /[(0/90) <sub>T</sub> ] <sub>3</sub>	20	4.2	79.5	1.6	1.0	1.6	68.4	42	81.3	116	83.34	0.718	5700	70.1
26	±15/0 <sub>2</sub> /±15	0	4.1	39.3	1.4	1.3	1.4	80.5	57	67.9	73.1	60.16	0.823	4843	71.3
27	±30/0 <sub>2</sub> /±30	0	3.8	39.3	1.3	1.2	1.3	81.2	59	56.1	58	42.92	0.740	3485	62.1
28	90 <sub>2</sub> /0 <sub>2</sub> /90 <sub>2</sub>	0	4.1	39.3	1.4	1.3	1.4	81.2	56	63.5	67	52.63	0.786	4274	67.3

Tab. 3. Properties of specimens made of a composite glass/epoxide

No of specimen	Structure	$\alpha$ [°]	t [mm]	$D_i$ [mm]	$t_i$ [mm]	$t_a$ [mm]	$t_o$ [mm]	h [mm]	z [%]	m [g]	$P_{max}$ [kN]	$P_a$ [kN]	$\frac{P_{max}}{P_{sr}}$	EA [J]	WEA [kJ/kg]
29	glass mat	0	3.5	39.3	-	-	-	86.7	35	59.4	52.6	43.8	0.833	3788	63.7
30	glass mat	0	9	39.3	-	-	-	91	35	168.3	137.4	117.7	0.857	10706	63.6
31	glass mat	5	2	60	-	-	-	91.2	35	35.9	20.7	16.6	0.802	1511	42.1
32	glass mat	5	2.7	61.6	-	-	-	93.2	35	65.7	47	39.2	0.834	3646	55.5
33	glass mat	5	4	61	-	-	-	91.1	35	100.1	70.2	59.5	0.848	5415	54.2
34	glass mat	5	5.2	59.6	-	-	-	92	35	123.4	88.4	75.6	0.855	6955	56.4
35	glass mat	10	1.5	61	-	-	-	82.3	35	31.7	18.9	15.6	0.825	1279	40.4
36	glass mat	10	1.8	62.4	-	-	-	85.2	35	36.5	26.1	20.2	0.774	1717	47.0
37	glass mat	10	2.3	60.4	-	-	-	86.3	35	46	34.3	24.9	0.726	2141	46.6
38	glass mat	10	3.2	60.6	-	-	-	91.9	35	68.4	54.7	42.1	0.770	3831	56.0
39	glass mat	10	4.2	60.6	-	-	-	91.7	35	81.4	72.6	56	0.771	5096	62.6
40	glass mat	10	5.5	61	-	-	-	84.3	35	111.4	99.7	80.8	0.810	6787	60.9
41	glass mat	15	3.4	59.2	-	-	-	62.6	35	48.4	56.9	41.8	0.735	2592	53.5
42	glass mat	15	4.2	59.6	-	-	-	62.3	35	59.9	69.1	54.7	0.792	3391	56.6
43	glass mat	15	5	60	-	-	-	62.5	35	73.9	88.3	67.6	0.766	4191	56.7
44	glass mat	15	6.4	60.2	-	-	-	62.4	35	99.2	132.3	98.5	0.745	6107	61.6
45	glass mat	20	2	80	-	-	-	70.8	35	45.5	27.5	18.6	0.676	1302	28.6
46	glass mat	20	4.2	80.6	-	-	-	70.2	35	92.4	77.5	59.2	0.764	4144	44.8
47	glass mat	20	8	79	-	-	-	64.2	35	162.3	175.5	143.5	0.818	9184	56.6
48	90/0 <sub>2</sub> /90	0	2.4	39.3	0.6	1.2	0.6	80.9	55	37.5	21.9	18.6	0.849	1597	42.6
49	(±45 <sub>T</sub> ) <sub>2</sub> /0 <sub>2</sub> /(±45 <sub>T</sub> ) <sub>2</sub>	0	3.4	39.3	1.1	1.2	1.1	90.1	49	53.4	34.1	31.7	0.930	2853	53.4
50	[±45 <sub>T</sub> ] <sub>2</sub>	0	1.4	39.3	-	-	-	59.9	45	20.0	13.8	11.0	0.797	659	32.9
51	[(0/90) <sub>T</sub> ] <sub>2</sub>	0	1.4	39.3	-	-	-	60.1	46	19.9	15.9	13.2	0.830	791	40.1
52	90/0/90	0	2	39.3	0.7	0.6	0.7	96	58	43.4	34.5	20.3	0.588	1953	45.0
53	90 <sub>2</sub> /0 <sub>2</sub> /90 <sub>2</sub>	0	3.7	39.3	1.2	1.3	1.2	89.8	56	84.8	62.5	51.0	0.816	4582	54.0
54	90 <sub>3</sub> /0 <sub>3</sub> /90 <sub>3</sub>	0	5.2	39.3	1.7	1.8	1.7	94.4	56	128.3	75.6	66.3	0.877	6260	48.8
55	[(0/90) <sub>T</sub> ] <sub>2</sub> /0 <sub>2</sub> /[(0/90) <sub>T</sub> ] <sub>2</sub>	0	4.5	39.3	1.5	1.5	1.5	94.7	49	79.8	66.8	62.7	0.939	5921	74.1
56	[(0/90) <sub>T</sub> ] <sub>4</sub> /0 <sub>4</sub> /[(0/90) <sub>T</sub> ] <sub>4</sub>	0	7	39.3	2.3	2.4	2.3	97.3	48	150.7	164.2	120.0	0.731	11680	77.4
57	(±45 <sub>T</sub> ) <sub>2</sub> /[(0/90) <sub>T</sub> ] <sub>2</sub> /(±45 <sub>T</sub> ) <sub>2</sub>	0	4.5	39.3	1.5	1.5	1.5	92.6	44	84.1	69.0	53.0	0.768	4895	58.4
58	±15/0 <sub>2</sub> /±15	0	4.5	39.3	1.5	1.5	1.5	99.1	55	97.3	50.2	41.0	0.817	4070	47.5
59	0 <sub>3</sub>	0	2.5	39.3	-	-	-	96.6	54	50.7	32.1	22.0	0.685	2126	41.9
60	90 <sub>3</sub>	0	3	39.3	-	-	-	80.7	55	60.3	32.8	23.0	0.701	1856	30.8
61	±30/0 <sub>2</sub> /±30	0	4.4	39.3	1.5	1.4	1.5	93.6	56	94.7	43.3	33.0	0.762	3085	32.6

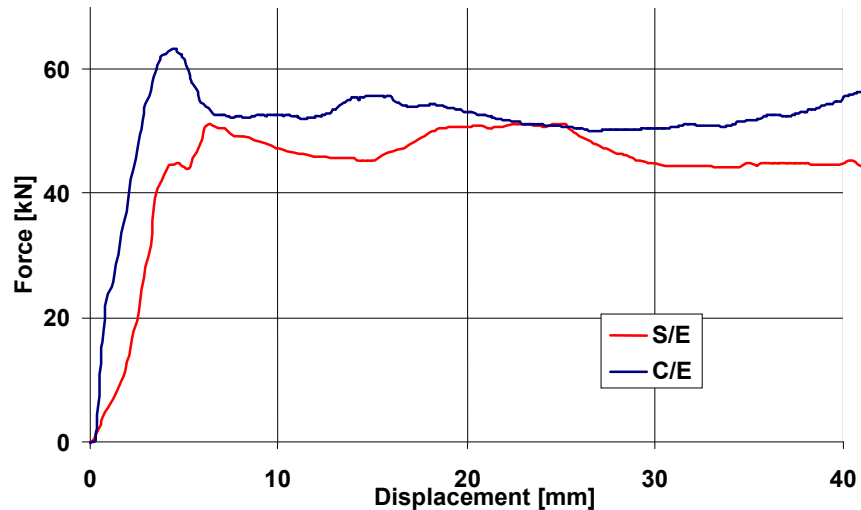


Fig. 8.  $P-\Delta$  dependence for pipes with  $\pm 15_2/0_2/\pm 15_2$  structure made of glass/epoxide and carbon/epoxide composite

Representative photos received during the test of composites strengthen with carbon and glass fibres at the progressive destruction of specimens are shown in Figs. 5, 6, and 9. In Fig. 9  $P-\Delta$  dependence, which is specified with a little distribution of results, is shown as an example.

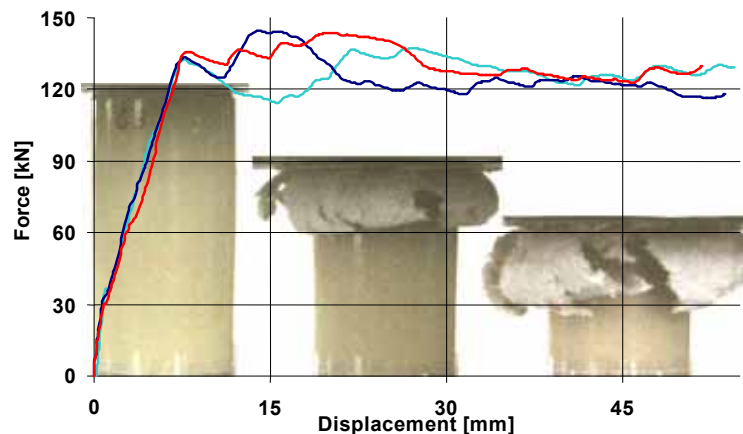


Fig. 9. Dependence of the destructive strength on displacement of 3 specimens of epoxide composite strengthen with glass mat

Results of tests concerning specimens in the shape of pipes, made of composite glass/epoxide and carbon/epoxide, showed that the greatest WEA have specimens whose external and internal layers are made of rowing material which take over the circumferential stresses, whereas, the external layers –from the rowing arranged parallel to the specimen's axis increase the bending strength. It is worth noticing that test results also showed that specimens strengthen with a glass mat appeared to have much greater ability to absorb energy.

#### 4. Mechanism of Destruction

Mechanism of destruction of fibre composites is difficult to describe because it depends mainly on the following factors: sort and shape of fibres, sort of a warp, an arrangement of fibres in a layer, a sequence of an arrangement, an angle of impact, a speed of loading, a shape of elements forming the construction absorbing energy and the content of fibres in a composite. During the progressive destruction the most frequent mechanisms of destruction were observed:

- destruction by transverse shearing
- destruction by brittle fracturing

- destruction by layer bending
- destruction by local buckling

Observations of the progressive destruction of specimens in the shape of pipes and truncated cones during tests suggest the destruction of specimens by layer bending with the simultaneous brittle cracking.

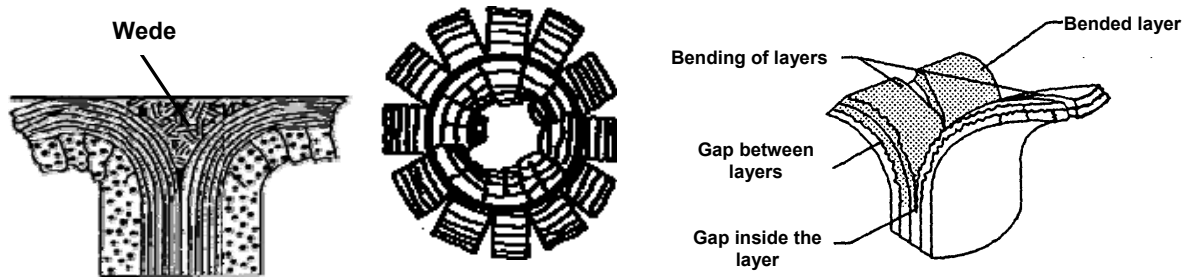


Fig. 10. Mechanism of destruction by layer bending after Ref. 3

The layer destruction by bending and crushing is characterized by very long interlayer and intralayer cracks parallel to fibres (Fig. 10).

In many works [1-6,8,10] it is considered that a composite is destroyed only or in a significant degree by bending. The main reason of appearing EA is an increase of warp cracking and first and foremost, the shape and an increase of interlayer cracks and a shape and an increase of cracks inside single layers. The cracks parallel to fibres propagate in the direction of fibres, inside a layer or inside separate layers with mutual oriented fibres. Two additional but no so important reasons of an increase of EA are connected with the specimen's friction which appears during the destruction of bending layer [1-3].

When the beam of layers is bended then the skid appears along the surface of the support of the testing machine. The friction appears also between layers which move between themselves during bending.

So, the increasing interlayer and intralayer cracks parallel to fibres and friction influence on the process of the destruction of bended layers. The propagation of cracks in bended layers and its mechanism is similar to the transverse shearing in which the length of cracks is of an order smaller. A wedge, supporting the layer bending, is created from a crushed resin (Fig. 10).

## 5. Influence of Factors on Ability of Absorbing Energy

From presented results in Tables 1 and 2 it is clearly seen that the sort of elements of a composite and the structure and the shape of specimens influence on EA. The special influence has the toughness of the resin, which hinders the development of cracks and thus increases WEA - Fig. 1.

On the basis of presented in Tables 2 and 3 results we can infer conclusions that parameters which essentially influence on bending and crushing in tests are: the sort of fibres strengthening the layer, the content of fibres in a composite, the fibre arrangement in a layer, the sequence of layer arrangement.

**Dependence EA on a composite thickness** is significant because the composite thickness influences on the bending strength which is indicated by the slope of the diagram visualising the dependence of the destructive force on the displacement in its initial state.

The greater thickness causes the greater rigidity of bending ( $EI$ ) which depends on the thickness in the third degree, as the result of it the force, necessary to receive the deformation, increases. The rigidity of bending depends, of course, on Modulus of Elasticity of longitudinal  $E$  which, on the other hand, depends on the sort and the structure of composites. In Fig. 11 the influence of the

composite thickness, strengthened with a glass mat, on the ability of absorbing energy is presented as an example.

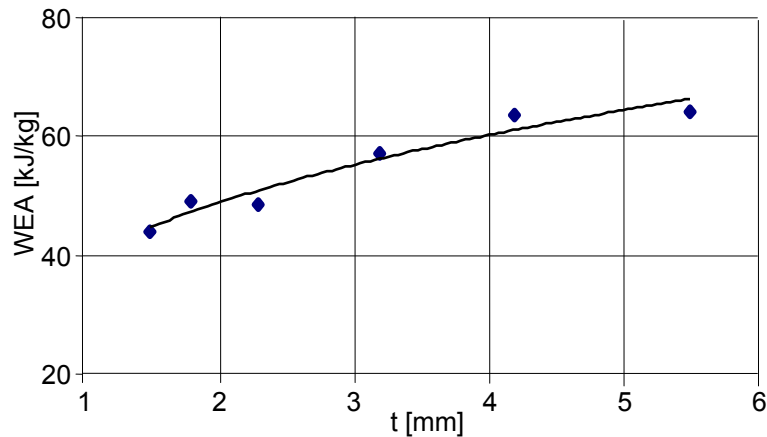


Fig. 11. Influence of the thickness of the cone wall on the ability of absorbing energy by the epoxide composite strengthened with a glass mat, for  $\alpha = 10^\circ$

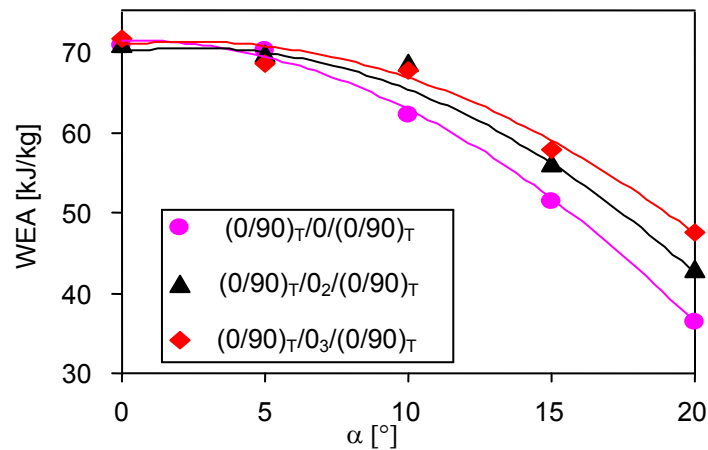


Fig. 12. Dependence of WEA on the angle  $\alpha$  for the chosen structures of composites (carbon/epoxide)

The influence of the fibre content in the composite decides about various mechanical properties of the composite which have an effect on bending and crushing of the specimen. The result of a higher content of fibres in the composite is its higher rigidity and strength of the fibre layer and the higher strength of the all composite. However, a very high content of fibres in a composite causes the lower fibre adhesion to the resin and therefore, the lower ability of absorbing energy.

**Fiber arrangement in the layer**, influence on mechanical properties, especially on the rigidity of bending, destructive deformations of tension and squeezing and the strength. The tests for the influence of the fibre arrangement in layers on the ability of absorbing energy showed that the best ability of absorbing energy has the composite of a structure  $(0/90)_T/0/(0/90)_T$ .

The results of tests on the influence of the half angle of the truncated cone on the EA value is presented in Fig. 12. From this figure it is seen that the highest ability of absorbing energy have the specimens with the angle equal to zero, the specimens in the shape of a pipe.

## 6. Conclusions

On the base of the literature review and our own tests concerning energy-consuming constructions it is possible to generalize the conclusion that polymer composites on account of their high mechanical properties with reference to a mass density, have a wide application in the construction of energy-consuming vehicles and space ships. The type of a composite and its

elements or a separator coating of the sandwich type have the influence on the value of absorbed energy. The energy-consuming constructions, especially made of composites, whose elements can take on various shapes, enable us to design constructions on the desired value of the absorbed energy and on the proper mechanism of the destruction of the construction during the collision, which ensure obtaining the high quality of the absorption energy.

Tests on specimens in the shape of pipes showed a great repeatability of results (Fig. 9) in the form of the dependence  $P_{\text{destr}} - \Delta l$ . The increase of WEA with the increase of the wall thickness, for taken to the tests composites and structures, may be used in the constructions requiring the absorption of a high energy. Circumferential oriented fibres, in specimens, have the main influence on lowering the quantity of interlayer cracks and their length which causes an increase of the absorbed energy. Specimens of the structure of  $[(0/90)_T/0_n/(0/90)_T]$ , strengthen with the continuous fibres showed, during the tests, the highest ability of absorbing the impact energy.

## References

- [1] Bannermann, D. C., Kinderwater C. M., *Crash Energy Absorption Properties of Composite Structural Elements*, High Performances Composite Materials New Applications and Industrial Production, G. Jube, A. Massiah, R. Naslain, M. Popot, eds., Soc. For the Advancement of Materials and Process Engineering, pp. 155-167, 1983.
- [2] Farley, Gary L., Jones, Robert M., *Crushing Characteristics of Continuons Fiber-Reinforced Composite Tubes*, Compos. Mater., vol. 26, pp. 37-50, 1992.
- [3] Farley, Gary L., Jones, Robert M., *Energy Absorption Capability of Composite Tubes and Beams*, NASA TM-101634, AVSCOM TR-89-B-003, 1989.
- [4] Hull, D., *Energy Absorption of Composite Materials Under Crash Conditions*, Progress in Science and Engineering of Composites-Proceedings of ICCM IV, T. Hayashi, K. Kawata, S. Umekawa, Pergamon Press, pp. 861-870, 1982.
- [5] Kinderwater, C. M., *Energy Absorbing Qualities of Fiber Reinforced Plastic Tubes*, National Specialists' Meeting on Composite Structures of the American Helicopter Soc., Philadelphia, 1983.
- [6] Mamalis A. G., Manolakos, D. E., Wiegelahn, G. L., *Crashworthy Behaviour of Thin-Walled Tubes of Fibre-glass Composite Materials Subjected to Axial Loading*, J. Compos. Mater., vol. 24, pp. 72-91, 1990.
- [7] Mamalis, A.G., Manolakos, D.E. & Viegelahn, G.L., *Crashworthy Characteristics of Thin Fibre-Reinforced Composite Frusta Under Axial Collapse*, International Journal of Vehicle Design, Vol. 10, pp. 165-174, 1989.
- [8] Ochelski S., *Metody doświadczalne mechaniki kompozytów konstrukcyjnych*, WNT Warszawa 2004.
- [9] Price, J.N., Hull, D. *The Crush Performance of Composite Structures*, Composite Structures, E.J. Marshall, Elsevier, pp. 2.32-2.44, 1987.
- [10] Thornton, P.H., *Energy Absorption in Composite Structures*, J. Compos. Mater., vol. 13, pp. 247-262, 1979.